A Local-Time Algorithm for Achieving Quantum Control†

Frank L. Yip, David A. Mazziotti,* and Herschel Rabitz

Department of Chemistry, Princeton University, Princeton, New Jersey 08544

Received: March 7, 2003; In Final Form: July 1, 2003

A local-time algorithm (LTA) is developed for designing electric fields to guide a quantum system toward a desired observable. The LTA is a noniterative forward marching procedure based on making a choice for the control field over the next immediate small time increment $t_{i+1} - t_i = \Delta$ solely on the ability of the local field value ϵ^i in that increment to take the system closer to the target goal. Each locally optimal field value ϵ^i, $i = 1, 2,...$ is chosen from a fixed toolkit of discretized members $\{\epsilon_j\}$ that sample the dynamic range $\epsilon_{min} \leq \epsilon \leq \epsilon_{max}$ of the control. Despite the strictly local myopic design process, the LTA is shown to be capable of achieving good quality control results in model systems. The LTA has no fixed time to reach the target, and the time it takes to produce good quality control primarily depends on the "distance" between the initial and target states, as measured by the number of intermediate state linkages connecting them and their strength. A comparison is made between the behavior of optimal control theory (OCT) and the LTA; each has different characteristics, and it is shown that the LTA can be computationally very efficient. LTA and traditional OCT methods can be viewed as extreme cases of a larger class of time-windowed approaches to control.

I. Introduction

Optimal control theory (OCT) provides a general framework for designing controls to manipulate quantum systems.[1−9] OCT operates by considering the initial state and desired final target observable value at target time T and searches for the optimal field $\epsilon(t)$ in an iterative manner over the time interval $0 \leq t \leq T$.[3,4] Importantly, OCT methods employ knowledge of the full dynamics of the system, including its future behavior, by exploring the entire time domain with simultaneous forward and backward time integration.

Such global approaches to field design have been demonstrated to generally give excellent results.[10−17] Previous work has been conducted to study the effectiveness of local optimization where the demand is often made that each step in time take the system closer to the objective.[5,18−22] Model predictive control breaks the full time interval $0 \leq t \leq T$ into a few or more time windows and seeks optimal performance in each window.[23−25] The extreme limit of the latter concept would be a local-time algorithm (LTA), which optimizes the system dynamics exclusively on the basis of the immediate local behavior over each successive small time step in the integration. This paper introduces a LTA where the field is developed through local decisions in time without considering any dynamic information beyond the present time step. The LTA is facilitated by discretizing the electric field amplitude $\epsilon_{min} \leq \epsilon \leq \epsilon_{max}$ into a typically small set of $2m + 1$ toolkit values $\{\epsilon_j\}$, $j = 1, 2, ..., 2m + 1$, from which the field is constructed. The field value ϵ^i over the ith time interval $t_{i+1} - t_i$ is selected to minimize the deviation of the observable $\langle O(t_i)\rangle$ and the target value O^*. The best choice among the $2m + 1$ possibilities is made at each time step with no hard demand of a monotonic approach to the target value O^* or that an imposed track be followed. The LTA benefits from its simplicity and avoidance of iteratively propagating the wave function. However, it is not a priori clear that strictly local control decisions can eventually lead to successful control possibly at some distant time in the future. However, this paper shows that the LTA can be effective under suitable conditions.

In this work, the LTA is developed for finite dimensional systems and illustrated for cases of dimensions 4 and 8. The issues that impact LTA behavior are discussed. Comparison to traditional OCT methods is also considered. Section II presents the LTA concept with illustrations given in Section III and concluding remarks given in section IV.

II. Formulation of the Local-Time Control Algorithm

The dynamical system is described by the time-dependent Schrödinger equation

$$i|\dot{\psi}\rangle = H(t)|\psi\rangle \equiv (H_0 - \mu\epsilon(t))|\psi\rangle \qquad |\psi(0)\rangle = |\psi_0\rangle \quad (1)$$

where H_0 is the free Hamiltonian of the system, μ is the dipole moment, and $\epsilon(t)$ is an external electric field. The propagtion of the system over the ith time step (all taken as uniformly spaced) on the interval $t_{i+1} - t_i = \Delta$ is given by a unitary operator U_i

$$|\psi(t_{i+1})\rangle = U_i|\psi(t_i)\rangle \quad (2)$$

with

$$U_i \equiv U(t_{i+1},t_i) \simeq \exp[-iH(t_i)\Delta] \quad (3)$$

where Δ is small enough to treat $H(t) \simeq H(t_i)$ over the interval. The LTA operates by making the best possible local choice for the propagator U_i with an eye only on the value $\langle O(t_i)\rangle = \langle\psi(t_{i+1})|O|\psi(t_{i+1})\rangle$ compared to the desired result O^* for the observable operator O.

Restricting the electric field in any time interval $t_{i+1} - t_i = \Delta$, $i = 1, 2, ...$ to be chosen from a small set of toolkit values facilitates the operation of the LTA. The toolkit is formed by discretizing the amplitude range $\epsilon_{min} \leq \epsilon \leq \epsilon_{max}$ into $2m + 1$

† Part of the special issue "Donald J. Kouri Festschrift".

* Corresponding author. E-mail: damazz@uchicago.edu.

10.1021/jp030313r CCC: $25.00
Published on Web 08/15/2003

equally spaced field values, defining the set

$$\{\epsilon_j\} = \{\epsilon_1, \epsilon_2, ..., \epsilon_{2m}, \epsilon_{2m+1}\} \quad (4)$$

where the integer m determines the level of resolution in the set $\{\epsilon_j\}$ that is constructed to be symmetric about $\epsilon_{m+1} = 0$. In practice, the set of field values is utilized to form a toolkit of propagation operators $\{\Omega_j\}$ where the jth member is $\Omega_j = \exp[-iH(t_j)\Delta]$.[26,27] Simple physical considerations can be employed to ensure that the field amplitude range $\epsilon_{\min} \leq \epsilon \leq \epsilon_{\max}$ is adequate for the control problem; the toolkit can easily be expanded if the dynamics warrants. Further requirements can be imposed on the decision at each time step to consider only particular field values from $\{\epsilon_j\}$ based on the desired degree of smoothness for the evolving field. The field value ϵ^i(or its associated propagator Ω^i) in the ith time step is chosen to move the system as close as possible to the target observable O^*,

$$\min_{\epsilon_i \in \{\epsilon_j\}} |\langle\psi(t_{i+1})| O |\psi(t_{i+1})\rangle - O^*| \equiv \min_{\Omega^i \in \{\Omega_j\}} |\langle\Omega^i\psi(t_i)| O |\Omega^i\psi(t_i)\rangle - O^*| \quad (5)$$

To carry out this optimization, the matrix element $\langle\Omega^j\psi(t_i)|O|\Omega^j\psi(t_i)\rangle$ is evaluated for the toolkit members $\{\Omega_j\}$ and the results scored in comparison to O^*. The winner Ω^i and its associated field value ϵ^i are recorded, and the process is then repeated at the text time step $t_{i+2} - t_{i+1} = \Delta$, etc., until the system is driven as close as possible toward the target O^*. No target time is specified, and the evolution is pursued as long as necessary. Given the local nature of the decision process, longer time evolution than for traditional OCT can be anticipated. However, no iteration is involved with just the added expense of testing the effectiveness of the toolkit members (typically a small set) at each time step. There is no guarantee that ϵ^i on the ith step will necessarily take the evolution closer to O^*; this possible nonmonotonic behavior is natural for quantum dynamics, including that found with OCT. The LTA can be viewed as seeking out the best of all possible local options, even when a particular choice may be negative in the sense that it can only take the system a bit further from O^* to cooperate with the dynamical capabilities of the system.

Unlike traditional OCT field design,[3−5] including methods that utilize the toolkit of propagators over the global time period,[26] the LTA operates with *no certain knowledge* of the future. All of the LTA decisions for field design are made *locally* at each time step with respect to the target observable. Nevertheles, the illustrations in section III show that despite the rather myopic view within the LTA it can still steer the dynamics step-by-step toward the target when given sufficient control time. The LTA examples below are chosen to demonstrate the general behavior of the method under different circumstances. A comparison will also be made between solutions from the LTA and those produced from traditional OCT and tracking.[27−30].

III. Illustrations

A. Local-Time Control for a 4-Level System. The model system considered has four nondegenerate levels and distinct transition frequencies with all of the initial population in the ground state $|1\rangle$.[31] The target goal is to occupy state $|4\rangle$ with a population of 0.95. All transitions, except the direct one $|1\rangle \rightarrow |4\rangle$, were allowed. Arbitrary units will be used in all of the following examples. The electric field amplitude is fixed to lie between $\epsilon_{\min} = -1$ and $\epsilon_{\max} = 1$. This amplitude range is discretized into 21 equally spaced increments of 0.1 between adjacent field values within $\{\epsilon_j\}$. The temporal step size is $\Delta = 0.1$. The final time is not fixed except through the criteria that it end when reaching the target population.

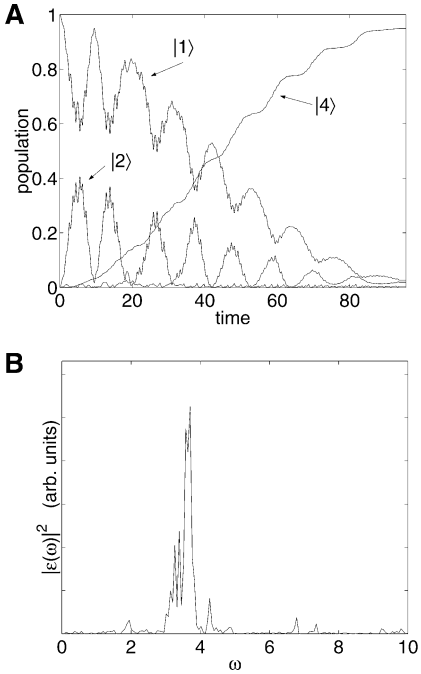

Figure 1. Local-time control with all 21 field values in $\{\epsilon_j\}$ considered. The amplitude was restricted to $[-1, 1]$ with a separation of 0.1 between neighboring field values. (A) Population oscillates primarily between $|1\rangle$ and $|2\rangle$ with diminishing amplitude as state $|4\rangle$ is populated monotonically over the control time. (B) The power spectrum of the field reveals a large cluster of frequencies near the $|1\rangle \rightarrow |2\rangle$ and $|2\rangle \rightarrow |4\rangle$ transitions at $\omega = 3$ and $\omega = 3.8$, respectively.

Figure 1A displays the controlled population evolution under the LTA when the local optimization in eq 5 is over all possible 21 toolkit values $\{\epsilon_j\}$ at each time step. The primary mechanism for reaching the target state is evidently the pathway $|1\rangle \rightarrow |2\rangle \rightarrow |4\rangle$ over the time interval of 93.5 (i.e., 935 time steps). The controlled behavior in Figure 1A is quite normal along with population of $|4\rangle$ rising a monotonic fashion. The field displayed a sinusoidal temporal structure (not shown here) including intervals when the field spanned the full allowed amplitude range available in the toolkit $\{\epsilon_j\}$. The power spectrum of this field is shown in Figure 1B. The most significant frequency structure appears between $\omega = 3$ and $\omega = 4$, which includes the $|1\rangle \rightarrow |2\rangle$ transition at $\omega = 3.0$ and the $|2\rangle \rightarrow |4\rangle$ transition at $\omega = 3.8$. In the LTA an analysis of the field frequency structure to assess mechanism is complicated by the local nature of the algorithm. The notion of frequency is a well-defined concept over a global time frame, and the local control decisions within the LTA will likely have difficulty clearly recognizing resonant absorption behavior. The LTA introduced some power at frequencies that do not correspond to the field-free transitions available to the system. This is reasonable because the local construction prevents the inclusion of a cost to minimize the field fluence, and dynamic power broadening can also permit deviations from resonant conditions. Because of the piecewise, discontinuous construction of the field from the toolkit, high-frequency structure is also present. Postfiltering the field to remove frequencies above $\omega = 6.0$ yields a field that is continuous and differentiable.[32] When this filtered field is integrated, the control shown in Figure 1A is reproduced.

A more restrictive approach to local-time design requires the field value ϵ^{i+1} at the time t_{i+1} to be close to the preceding

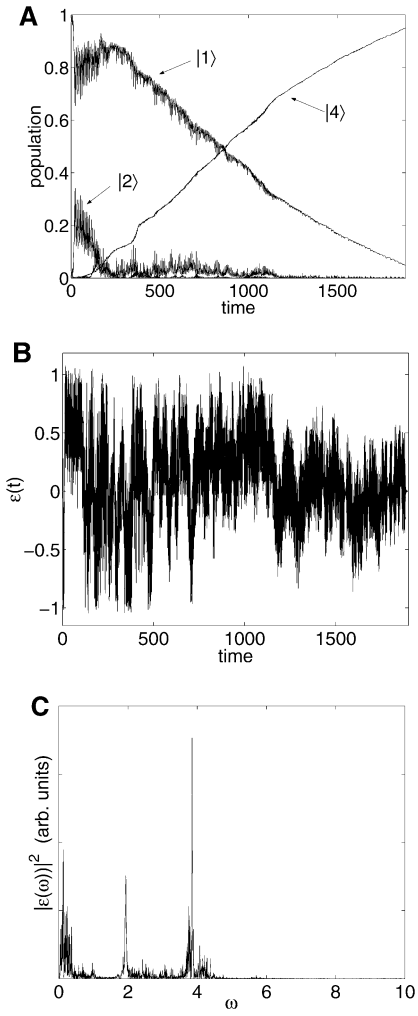

Figure 2. Local-time control with only nearest-neighboring field values considered at each time step. The amplitude was restriced to [−1, 1] with a separation of 0.1 between neighboring field values. (A) Population moves from $|1\rangle$ to $|2\rangle$ and oscillates between these states. The population of state $|4\rangle$ is not monotonic in its fine detailed evolution. The electric field (B) and corresponding power spectrum (C) show complex oscillating structure. A band-pass filter with a cutoff beyond the system transition frequencies was used to smooth the digital nature of the toolkit field variation; the controlled dynamics was invariant to this operation.

field value ϵ^i at time t_i to prevent large amplitude jumps within small time frames. For example, if $\epsilon^i = \epsilon_k$, where ϵ_k is the optimally chosen value from the toolkit $\{\epsilon_j\}$, then ϵ^{i+1} may be restricted to lie among the nearest-neighbor values ϵ_{k+1}, ϵ_k, or ϵ_{k-1}. This nearest-neighbor condition was imposed on the 4-level system. The dynamics for this example are shown in Figure 2A. The target was achieved in 18 830 steps. The much longer required time for the dynamics in this case compared to the last one is consistent with the imposition of restrictions on the local field decisions (see section III.B below). The mechanism is again dominated by the $|1\rangle \rightarrow |2\rangle \rightarrow |4\rangle$ transition. Although the overall population of $|4\rangle$ appears to rise monotonically, many intermediate steps took small increments away from the target. This behavior is indicative of an "intelligent" algorithm that recognizes that reaching the target also requires working cooperatively with the dynamical capabilities of the system. The field produced by the LTA is shown in Figure 2B. Figure 2C displays the corresponding power spectrum. A more intense and complex frequency structure is present in this case than in the previous example, including significant low-frequency components.

TABLE 1: Time Steps Required To Achieve Control[a]

	field resolution		
subset of fields for control decisions	$m = 5$, $\lvert\epsilon_j - \epsilon_{j\pm1}\rvert = 0.2$	$m = 10$, $\lvert\epsilon_j - \epsilon_{j\pm1}\rvert = 0.1$	$m = 20$, $\lvert\epsilon_j - \epsilon_{j\pm1}\rvert = 0.05$
$\{\epsilon_{j-1}, \epsilon_j, \epsilon_{j+1}\}$	1719	18830	66532
$\{\epsilon_{j-2}, ..., \epsilon_{j+2}\}$	1093	1887	15685
$\{\epsilon_{j-3}, ..., \epsilon_{j+3}\}$	1109	1800	10016
$\{\epsilon_j\}$, $j = 1, 2, ..., 2m + 1$	986	935	989

[a] Number of time steps required to achieve the target population of $|4\rangle$ with the LTA. The amplitude range is fixed between $\epsilon_{min} = -1$ and $\epsilon_{max} = 1$. When the subset is restricted to less than the full set $\{\epsilon_j\}$, $j = 1, 2, ..., 2m + 1$, the algorithm requires a longer time to achieve the target as the amplitude spacing decreases. The last row shows that total freedom in choosing a field value, regardless of the field resolution, allows the algorithm to achieve the target with essentially the same effort.

B. Influence of Toolkit $\{\epsilon_j\}$ Resolution Decision Constraints in the Algorithm. The examples in Figures 1 and 2 illustrate how constraints on the local field decisions can affect the dynamics and especially the number of time steps needed to reach the target. This point will be explained further here through consideration of transition rules that restrict the field choices (e.g., nearest-neighbors, next-nearest-neighbors, etc.) at each time step. The level of vertical resolution (i.e., the amplitude separation between adjacent field values) of $\{\epsilon_j\}$ also can impact the amount of time required to reach the target goal. To consider these matters, Table 1 displays the number of time steps required to reach the target under various conditions. In the table the full range of the field amplitude is $-1 \leq \epsilon \leq 1$. For cases where the number of field values to choose from is restricted at each time step, the time required to reach the control objective increases as the spacing between the toolkit members $|\epsilon_j - \epsilon_{j-1}|$ decreases. Furthermore, as the subset of field values at each time step becomes less restrictive, the time necessary to achieve the target decreases. For the fully flexible cases where the entire set of amplitude values $\{\epsilon_j\}$ can be considered (i.e., see the last row in Table 1), the time required for control was similar and relatively invariant to the amplitude resolution (i.e., different m values). All of the observations in Table 1 are consistent with the simple consideration that added freedom in choosing the field at each time step tends to decrease the effort in reaching the target.

C. Local-Time Control for an 8-Level System. The four-level system was expanded to include a total of eight nondegenerate levels[33] with unique transition frequencies. Single transitions beyond three energy levels were forbidden. The target in this case was to move population from $|1\rangle$ to $|8\rangle$. The electric field amplitude and discretization were the same as described in section III.A. The control results will be described here without figures, as the qualitative behavior was similar to that indicated in Figures 1 and 2. For the restrictive case where only nearest-neighboring electric field values were considered at each time step, the population in state $|8\rangle$ was 0.09 after 50 000 steps with only slow change in the dynamics beyond that point. Allowing the algorithm to consider the entire toolkit $\{\epsilon_j\}$ of 21 field values to choose from at each time step increased the population of $|8\rangle$ to 0.76 after 50 000 steps, with the remaining population mostly in $|2\rangle$ and $|4\rangle$. The field showed significant low-frequency structure, and postfiltering this low frequency severely reduced the level of control. From the results in Table 1, the performance would improve by permitting more flexibility through a larger dynamic range in the toolkit $\{\epsilon_j\}$.

Permitting a very weak direct transition between $|1\rangle$ and $|8\rangle$ allowed for population of greater than 0.9 to be reached in $|8\rangle$

for each of the cases above. Again, population reached the target state in less time when the algorithm was given more flexibility in choosing a field value. The dominant frequency in the fields occurred for the $|1\rangle \rightarrow |8\rangle$ transition. Thus, the LTA was able to populate a distant state most efficiently when a direct path was available. This behavior is consistent with the operation of the LTA, which is best suited for situations where the local control decisions can have a clear, direct impact on the target. This is a restriction in the use of the LTA, but even in this example, it was able to significantly populate a distant state when sufficient freedom was allowed at each local time step.

D. Comparison of Local-Time Control with OCT. Because OCT is a benchmark for achieving control designs for arbitrary controllable quantum systems, it is instructive to compare the control performance of the LTA with that of OCT. The test conditions are carried out for the 4-level system described in section III.A.

For the OCT case, the cost functional included a modest fluence term[3,4] and the time domain was fixed to 10 000 time steps of size $\Delta = 0.1$ (i.e., the target time was $T = 1000$). The initial field introduced into the OCT algorithm was $\epsilon(t_k) = 0$, for all $k =$ values. After 141 iterations, the target of 0.95 population in $|4\rangle$ was achieved. The population dynamics indicate a mechanism of $|1\rangle \rightarrow |2\rangle \rightarrow |4\rangle$ similar to the LTA dynamics. However, the detailed dynamics in the OCT and the two LTA cases was quite different. The LTA dynamics show some small population in $|3\rangle$ and more complex frequency structure within the control fields.

To compare the relative cost of the LTA versus the OCT algorithms for these examples, we will compute the ratio r of the number of mathematical operations needed to reach the target for the OCT algorithm to that of the LTA (i.e., $r =$ OCT/LTA operational costs). For the example in Figure 1 the ratio was $r = 64$ and for the case in Figure 2, $r = 11$, showing good efficiency for the LTA. The restricted choices available to the LTA in Figure 2 alone would decrease the number of LTA operations; however, the added time to reach the target more than compensated for that savings to give a net increase in the LTA cost in that case. The main source of the LTA efficiency is its operation without costly iteration whereas OCT generally cycles through repeated calculations many times before convergence is achieved. Similar behavior was also found in other cases where OCT and LTA both reached the target value. Although the results are interesting, it must be stressed that a direct comparison between OCT and LTA calls for considerable caution. Each method operates under fundamentally different conditions, often producing qualitatively different control fields and mechanisms. OCT produces temporally optimal solutions (i.e., after even the first iteration the new field at any time t_i is influenced by controlled dynamics over the full time interval $0 \leq t \leq T$) by evaluating global considerations that are not possible to implement in the LTA. The results in this paper are not presented to intimate that LTA can replace tradtional OCT methods. Rather, the comparison with OCT illustrates that the LTA operates in a unique fashion with different consequences for the controlled dynamics, yet with some efficiency and capabilities despite the very limited information included in the local learning algorithm.

IV. Concluding Remarks

Fully local-time design by the LTA is appealing because of the simplicity of the algorithm and the minimal amount of information required for its operation. This paper shows that such a simple procedure operating with a very myopic decision process often still can find successful controls. Unlike OCT,[3−5,8] the LTA fields are not explicitly tailored by cost functionals that include global temporal information. Rather, the LTA technique constructs fields at each time step without knowledge of the system's future dynamics. An example of this distinction is the way each method minimizes the energy of the field. OCT often requires minimum input energy by placing appropriate costs on the fluence of the field. The LTA, however, simply requires that the field amplitude remains within some modest bound. The computational costs associated with the LTA benefit from the lack of iteration while achieving control. The degree of control flexibility arising from discretization of the electric field amplitude $\epsilon_{\min} \leq \epsilon \leq \epsilon_{\max}$ affects the operation of the LTA. The LTA will operate best when the target is near the initial state in the sense of there being a relatively small number of strongly coupled intermediate states linking them.

Although LTA and OCT methods differ fundamentally in the scope and nature of information used to design the control field, the LTA is closely related to tracking methods in optimal control.[27−30] Tracking problems involve searching for a control field that produces dynamics that follow a prescribed path. A central issue in tracking is the avoidance of singularities that may occur while attempting to adhere to the track. Utilizing a local-time construction with the toolkit of field values is appealing for tracking because it can completely avoid singularities while attempting to stay as close as possible to the imposed track.

The LTA determines a field that drives the system toward the target, although not likely in a global temporal sense as with OCT. The LTA is an optimal control procedure where the field is chosen as optimal separately over each small time window for its (future) impact on reaching the target. The LTA and traditional OCT can be considered as optimal control procedures operating at the two extreme time window limits. In the same manner, by extending the time window for consideration the LTA may be morphed to become OCT in the global limit. A full family of time-windowed local approaches[21−23] lies between these limits. Tradeoffs likely exist in considering the simplicity of the local methods to the increasing globality of the windowed methods. This paper shows that control may be achieved even when operating at the smallest time steps (windows) to make field choices.

Acknowledgment. We acknowledge support from the National Science Foundation and the Department of Defense.

References and Notes

(1) Rabitz, H.; de Vivie-Riedle, R.; Motzkus, M.; Kompa, K. *Science* **2000**, *288*, 824.
(2) Rice, S. A.; Zhao, M. *Quantum Control of Molecular Dynamics*; Wiley-Interscience, New York, 2000.
(3) Shi, S.; Rabitz, H. *J. Chem. Phys.* **1990**, *92*, 364.
(4) Rabitz, H.; Zhu, W. *Acc. Chem. Res.* **2000**, *33*, 572.
(5) Kosloff, R.; Rice, S. A.; Gaspard, P.; Tersigni, S.; Tannor, D. J. *Chem. Phys.* **1989**, *139*, 201.
(6) Pierce, A. P.; Dahleh, M. A.; Rabitz, H. *Phys. Rev. A* **1988**, *37*, 4950.
(7) de Vivie-Riedle, R.; Sundermann, K.; Motzkus, M. *Faraday Discuss.* **1999**, *113*, 303.
(8) Geremia, J. M.; Zhu, W.; Rabitz, H. *J. Chem. Phys.* **2000**, *113*, 10848.
(9) Zhu, W.; Rabitz, H. *J. Chem. Phys.* **1999**, *109*, 385.
(10) Hoki, K.; Fujimura, Y. *Chem. Phys.* **2001**, *267*, 187.
(11) Sundermann, K.; de Vivie-Riedle, R. *J. Chem. Phys.* **1999**, *110*, 1896.
(12) Kaluža, M.; Muckerman, J. T.; Gross, P.; Rabitz, H. *J. Chem. Phys.* **1994**, *100*, 4211.
(13) Manz, J.; Sundermann, K.; de Vivie-Riedle, R. *Chem. Phys. Lett.* **1998**, *209*, 415.

(14) Judson, R. S.; Rabitz, H. *Phys. Rev. Lett.* **1992**, *68*, 1500.
(15) N. Došlić, Kühn, O.; Manz, J.; Sundermann, K. *J. Phys. Chem. A* **1998**, *102*, 9645.
(16) Zhang, H.; Rabitz, H. *Phys. Rev. A* **1994**, *49*, 2241.
(17) Zhu, W.; Rabitz, H. *J. Phys. Chem. A* **1999**, *103*, 10187.
(18) Ohtsuki, Y.; Yahata, Y.; Kono, H.; Fujimura, Y. *Chem. Phys. Lett.* **1998**, *287*, 627.
(19) Tannor, D. J.; Kosloff, R.; Bartana, A. *Faraday Discuss.* **1999**, *113*, 365.
(20) Sugawara, M.; Fujimura, Y. *J. Chem. Phys.* **1994**, *100*, 5646.
(21) Ohtsuki, Y.; Kono, H.; Fujimura, Y. *J. Chem. Phys.* **1998**, *109*, 9318.
(22) Watanabe, Y.; Umeda, H.; Ohtsuki, Y.; Kono, H.; Fujimura, Y. *Chem. Phys.* **1997**, *217*, 317.
(23) De Nicolao, G.; Magni, L.; Scattolini, R. *Lect. Notes Contr. Inf.* **1999**, *245*, 408.
(24) Mayne, D. Q.; Rawlings, J. B.; Rao, C. V.; Scokaert, P. O. M. *Automatica* **2000**, *36*, 789.
(25) Mayne, D. Q.; Schroeder, W. R. *Automatica* **1997**, *33*, 2103.
(26) Yip, F.; Mazziotti, D.; Rabitz, H. *J. Chem. Phys.* **2003**, *118*, 8168.
(27) Lu, Z. M.; Rabitz, H. *J. Phys. Chem.* **1995**, *9*, 13731.
(28) Chen, Y.; Gross, P.; Ramakrishna, V.; Rabitz, H.; Mease, K. *J. Chem. Phys.* **1995**, *102*, 8001.
(29) Nguyen-Dang, T. T.; Chatelas, C.; Tanguay, D. *J. Chem. Phys.* **1995**, *102*, 1528.
(30) Magni, L.; De Nicolao, G.; Scattolini, R. *Automatica* **2001**, *37*, 1601.

(31) The eigenvalues of H_0 for the four levels were 1.0, 4.0, 6.0, and 7.8. The coupling between the levels was as follows: $\mu_{12} = 0.30$, $\mu_{23} = 0.25$, $\mu_{34} = 0.15$, $\mu_{13} = 0.09$, $\mu_{24} = 0.08$, and $\mu_{14} = 0.00$.

(32) Low-pass postfiltering was accomplised by fast Fourier transforming (FFT) the electric field signal, setting all frequencies above a cutoff value equal to zero, and finally inverse fast Fourier transforming the data back into the time domain. Details of postfilter implementation can be found in: Mitra, S. K. *Digital Signal Processing: A Computer Based Approach*; McGraw-Hill: New York, 2000.

(33) The specifications for the levels $|1\rangle$ through $|4\rangle$ were the same as the example in section III.[31] The eigenvalues for levels $|5\rangle$ through $|8\rangle$ were 8.42, 9.00, 9.48, and 9.78, respectively. Nonzero coupling elements of μ were 0.15 between adjacent levels, 0.08 for next-nearest-neighbor transitions, and 0.01 for transitions through two intermediate states.